Synaptic Distinction of Laminar-specific Prefrontal-temporal Pathways in Primates

Michael Germuska[1], Subhash Saha[2], John Fiala[3] and Helen Barbas[2,4,5]

[1]Department of Biomedical Engineering, Boston University and School of Medicine, Boston, MA, USA, [2]Department of Health Sciences, Boston University and School of Medicine, Boston, MA, USA, [3]Department of Biology, Boston University and School of Medicine, Boston, MA, USA, [4]Department of Anatomy and Neurobiology, Boston University and School of Medicine, Boston, MA, USA and [5]Program in Neuroscience, Boston University and School of Medicine, Boston, MA, USA

Prefrontal pathways exert diverse effects in widespread cortical areas, issuing projections both to the middle layers and to layer I, which are anatomically and functionally distinct. Here we addressed the still unanswered question of whether cortical pathways that terminate in different layers are distinct at the synaptic level. We addressed this issue using as a model system the robust and functionally significant pathways from prefrontal areas 10 and 32 to superior temporal areas in rhesus monkeys. Boutons from prefrontal axons synapsing in the middle layers of superior temporal cortex were significantly larger than boutons synapsing in layer I. Most synapses were on spines in both layers, which are found on dendrites of excitatory neurons. The less prevalent synapses on smooth dendrites, characteristic of inhibitory interneurons, were more common in the middle cortical layers than in layer I. Bouton volume was linearly related to vesicular and mitochondrial content in both layers, though a subset of small boutons, found mostly in layer I, contained no mitochondria. The systematic laminar-specific pre-synaptic differences in stable cortical synapses in adult primates were independent of their origin in the functionally distinct prefrontal areas 10 and 32, or their destination in architectonically distinct superior temporal areas. This synaptic distinction suggests differences in efficacy of synaptic transmission and metabolic demands in laminar-specific pathways that may be selectively recruited in behavior.

Keywords: anterior cingulate, auditory association cortex, laminar distinction, laminar pathways, presynaptic features, synaptic efficacy

Introduction

The prefrontal cortex in primates has widespread connections with sensory and other association cortices (reviewed in Barbas *et al.*, 2002). Global access to information is necessary for the executive functions of the prefrontal cortex, but for any given task the information retrieved must be specific. An important way to endow specificity to cortical pathways is by termination in distinct layers, where neurons have specific inputs and outputs, and specific chemical and physiologic properties (Lund, 1988; Hof *et al.*, 1999).

An unanswered question is whether prefrontal pathways that terminate in different layers are distinct at the synaptic level. We have addressed this issue using the functionally significant and anatomically robust pathway from prefrontal cortex to superior temporal cortex as a model system. We focused on pathways that originate in prefrontal areas 10 and 32 and terminate in overlapping areas and layers of superior temporal cortex. Both prefrontal areas are robustly connected with superior temporal auditory association areas, but are otherwise distinct (reviewed in Barbas *et al.*, 2002). Area 32 in the anterior cingulate has a key role in species-specific vocalization (reviewed in Vogt and

Barbas, 1988). On the other hand, lateral prefrontal areas, such as area 10, have a role in cognitive tasks, including extracting relevant auditory signals from noise and in specialized working memory tasks (e.g. Chao and Knight, 1997, 1998; Koechlin *et al.*, 1999). The termination in auditory association areas of pathways from areas 32 and 10 may thus have distinct functions within the auditory modality.

We therefore investigated and compared the structural synaptic features of prefrontal pathways as they terminate in the middle layers (IV–upper V) and in layer I of superior temporal cortex. These layers differ markedly in their connections and functions. The middle cortical layers are targets of 'forward' projections from other cortical areas, whereas layer I is the target of cortical 'feedback' projections (reviewed in Felleman and Van Essen, 1991). This model pathway system allowed us to address several questions: Are the synaptic features of prefrontal pathways similar or different when they terminate in layer I versus layers IV–upper V? Do synaptic features vary depending on the specific prefrontal origin, or the specific site of termination within superior temporal cortex? We provide evidence of systematic differences in prefrontal pathways terminating in distinct layers of superior temporal cortex. Prominent differences at the synaptic level have important implications on synaptic efficacy of laminar-specific pathways, and raise questions on selective recruitment of components of these pathways in behavior.

Materials and Methods

Subjects
Experiments were conducted on five rhesus monkeys (*Macaca mulatta*) of both sexes, 1-3 years of age, grouped by the tracer injection site in prefrontal cortices as follows: Tracer injection in area 32: cases AY (female, 3 years); BG (female, 2 years). Tracer injection in area 10: cases BF (female, 2 years); BA (male, 1 year); BC (male, 3 years).

Surgical Procedures
The monkeys were anesthetized with ketamine hydrochloride (10-15 mg/kg, i.m.) followed by isoflurane anesthetic until a surgical level of anesthesia was accomplished. The monkeys were then placed in a stereotaxic apparatus and a small region of the prefrontal cortex was exposed. Surgery was performed under aseptic conditions while heart rate, muscle tone, respiration and pupillary dilatation were closely monitored.

Injection of Neural Tracers
Injections of biotinylated dextran amine (BDA, Molecular Probes, Eugene, OR) were placed in prefrontal areas 10 and 32 in different animals. The dye concentration was 10 mg/ml, and was injected in volumes of 3-4.5 µl in three cases (AY, BA, BC) and 10 µl in two cases (case BF, BG) using a microsyringe (Hamilton, Reno, NV) mounted on a microdrive. We used the 10 000 mol. wt form of BDA, known to be

optimal for anterograde but not retrograde labeling (e.g. Veenman *et al.*, 1992; Reiner *et al.*, 2000; and personal observations). This form of BDA labels the entire extent of axonal terminals and boutons. In each case, the dye was delivered in 2-4 penetrations at a depth of 1.2-1.6 mm below the pial surface. For each injection the needle was left *in situ* for 10-15 min, to allow local diffusion of dye at the injection site and prevent upward diffusion of the dye upon retraction of the needle.

Perfusion and Tissue Processing
The survival period was 18 days. The animals were then anesthetized with a lethal dose of sodium pentobarbital (>50 mg/kg, to effect) and perfused with 4% paraformaldehyde, 0.2% glutaraldehyde in 0.1 M phosphate buffer (pH 7.4). The brain was removed from the skull, photographed and placed in graded solutions of sucrose (10-30% in 0.1 M PBS) for cryoprotection.

Brains were frozen in –75°C isopentane (Fisher), according to the protocol of Rosene *et al.* (1986) and cut on a freezing microtome in the coronal plane at 50 μm to produce 10 series per hemisphere. Two adjacent series of sections were processed to visualize labeled boutons in superior temporal cortices. Sections were washed in 0.1 M PBS and placed in avidin–biotin complex solution (Vector Laboratories, Burlingame, CA) overnight. Sections were then washed and processed with diaminobenzidine (DAB, Zymed Laboratories, San Francisco, CA). One series of sections was mounted, dried, and every other section Nissl stained for mapping at the light microscope. Tissue sections from a matched series through the superior temporal gyrus were mounted, viewed while wet, and small regions with label were cut, postfixed in 0.5% osmium tetroxide in 0.1 M phosphate buffer for 3 min, dehydrated through graded ethanol and propylene oxide, and embedded in Araldite between two sheets of Aclar plastic film. Photographs of the sections were captured with a CCD camera using a software system (Neurolucida, Colchester, VT).

For ultrastructural examination, pieces of tissue with label were cut from superficial layer I, which is largely cell-free and easy to distinguish. Pieces from the middle layers included the distinguishable layer IV and the immediately adjacent upper part of layer V. The tissue was mounted on Araldite blocks by high-strength, rapid-bonding adhesive α-cyanoacrylate (Aron Alpha 201, Ted Pella Inc.. CA). Ultrathin (70 nm) sections were cut with a diamond knife (Diatome, Fort Washington, PA) on an ultramicrotome (Leica Ultracut UCT, Leica Wien, Austria) and sections were collected on single slot grids coated with Pioloform. For serial reconstruction sections were cut in uninterrupted series of 60-120 sections at 50 nm. The sections were counterstained with uranyl acetate and lead citrate.

Sampling Size
For single section analysis 1-4 pieces of tissue were cut from layer I from each case (total = 8 in 5 cases), and 1-3 pieces from the middle layers (total = 8 in 5 cases), representative of the labeling in area Ts1 (cases AY, BG, BC, BA), or in area Ts3 (case BF). The sites sampled from architectonic area Ts1 were matched for rostro-caudal level across cases (cases AY, BG, BC, BA), and included the entire segment with label at the matched level of Ts1. The average size of the pieces for ultrathin sectioning after trimming was 430 × 550 μm. The average size of tissue from layer I (300 × 400 μm) was smaller than for the middle layers (500 × 650 μm), because the density of labeling in the superficial layers was higher than the middle layers, as reported in a previous study (Barbas *et al.*, 2005). From each piece of tissue, six adjacent ultrathin sections were obtained at intervals of 1 μm throughout the thickness of the section (50 μm). Triplets of adjacent sections were mounted on two separate grids. One grid was used for analysis and the other was saved as a spare series in case of damage to a grid during viewing at the electron microscope. The three adjacent sections were used to help make a positive identification of synaptic features, and sampling every 1 μm ensured that synapses were not counted twice. This systematic sampling yielded an average of 185 ultrathin sections from each piece of tissue available for analysis, half of which were back-up sections. An average of 38% of all ultrathin sections prepared were viewed using exhaustive sampling, so that all labeled boutons in each section examined were photographed and analyzed, as described below.

For serial section analysis pieces of tissue from layer I ($n = 2$) were an average of 90 × 230 μm, and for the middle layers ($n = 2$) they averaged 125 × 250 μm (cases BC and BF). For layer I we performed exhaustive analysis of all labeled boutons from an average of 106 sections from each case (case BC, 100 sections; case BF, 113 sections), and from an average of 178 sections through the middle layers (case BC, 183 sections; case BF 173 sections).

Data Analysis
Ultrathin sections were examined with a JEOL CX100 electron microscope. BDA-labeled terminals forming synapses were photographed at 10 000× or 6500× and the negatives were scanned (Minolta Dimage Scan Multi II scanner). We used classic criteria to identify synapses and profiles (Peters *et al.*, 1991): aggregation of synaptic vesicles in the presynaptic bouton, rigid apposition of the presynaptic and postsynaptic membranes and associated widening of the extracellular space; and the presence of pre- and postsynaptic membrane specializations. Asymmetric synapses (type I) were classified by thickened postsynaptic densities and rounded vesicles; and symmetric (type II) synapses by thin postsynaptic densities and pleomorphic vesicles. Dendritic shafts contain mitochondria, microtubules and endoplasmic reticulum, while profiles lacking these organelles were identified as dendritic spines. In optimal sections through spines it is possible to see the spine apparatus (reviewed in Fiala and Harris, 1999).

Two-dimensional (2D) Analysis
We conducted exhaustive systematic search of the prepared grids, so that all labeled boutons and the corresponding postsynaptic sites were photographed for each case, until about 100 synapses were photographed from each layer for each case. Because labeling in layer I was denser than in the middle layers, a larger amount of tissue had to be used from the middle layers to yield a comparable sample. We measured the cross-sectional area of BDA axon terminals using an image analysis system (Metamorph, Universal Imaging, West Chester, PA). In addition, we measured bouton area of unlabeled axonal terminals forming synapses in a random sample averaging one in five of the frames that included labeled synapses (frame dimension 8.3 ×14 μm), to investigate if the population of labeled boutons was representative of, or differed from, the local population of boutons.

Three-dimensional (3D) Analysis
We used series of 30-50 uninterrupted sections to reconstruct labeled boutons and their postsynaptic spines. We used the freeware program sEM Align to correct for the misalignments between images of sections caused by serial sectioning and scanning of the tissue (Fiala and Harris, 2002). The dimensions of the scanned images were calculated by comparison with an image of a diffraction grating. The thickness of the image sections was calculated using the method of cylindrical diameters (Fiala and Harris, 2001).

After calibration, boutons, mitochondria, spines and postsynaptic densities were reconstructed using IGL Trace (www.synapses.bu.edu). Object contours were manually traced section-by-section, and the program was used to generate a 3D Virtual Reality Modeling Language (VRML) object, which implicitly contains such information as volume and surface area.

Vesicle measurements
We counted vesicles in a random sample of labeled boutons ($n = 24$) from layer I and from layers IV–V using random systematic sampling of five boutons and skipping five, resulting in standard error of less than 5%. From this sample, we counted all vesicles within every section profile of each reconstructed bouton. Using the vesicle diameter and section thickness we made estimates of true vesicle counts using Abercrombie's correction factor, $N = n[T/(T + D)]$, where N is the 'true' count, n the actual number counted, T the tissue thickness, D the mean diameter of vesicles (Abercrombie, 1946). The Abercrombie correction factor was necessary to avoid over counting, since D in this case was a significant proportion of T (~50%), and because it was not possible to match profiles of transected vesicles across sections (for discussion see Guillery and Herrup, 1997). The Abercrombie correction is appropriate

for counting spherical objects (for discussion see Abercrombie, 1946; Schmitz and Hof, 2005), such as synaptic vesicles in excitatory synapses (Peters *et al.*, 1991). Vesicle diameters were measured in a systematic random sample of labeled boutons in layer I and layers IV–V. Measurements of vesicular diameter were made from a sample of 200 vesicles in each layer, which constitutes an adequate sample as recommended by Fox (1988). To account for diameter measurements made on vesicles that did not pass through their equator, corrections were made according to the method proposed by Froesch (1973).

Statistics

We used the Matlab Statistics Toolbox for statistical analyses. In each case a significance level of $P < 0.05$ was used. Probability density estimate (PDE) of the volume of all boutons was obtained by nonparametric Gaussian smoothing. The PDE is estimated by placing a Gaussian kernel function on each data point and averaging the Gaussian densities at each point. This method does not assume that the PDE has a specific form, and allows its shape to be entirely determined from the data (Archambeaum and Verleysen, 2003).

Results

Data were obtained after tracer injections in prefrontal cortices in five rhesus monkeys, as shown on a composite of the injection sites in Figure 1. In all cases the injection sites were confined to the cortical mantle and included all cortical layers. In two cases the injection was in area 32 (cases AY, BG), and in three in area 10, including its rostral (case BA) and caudal (cases BC, BF) parts. In one of the latter cases, the injection included a small part of adjacent area 9 (case BC). The size of the injection sites is shown in Figure 1. The rostrocaudal extent of the injection sites ranged from 0.7 mm (case AY) to 2.1 mm (case BC).

Identified boutons belonging to axons emanating from area 32 terminated in anterior superior temporal cortices (the temporal pole and areas Ts1 and Ts2), and to a lesser extent in posterior superior temporal cortex (parainsular area and area Ts3). A similar pattern was seen for rostral area 10 (case BA). Projections from caudal area 10 extended more caudally, within auditory association area Ts3, as well as in areas Ts1 and Ts2 (cases BF, BC). Axons from area 32 and from area 10 terminated in both superficial and middle-deep layers, and overlapped topographically and in several layers of superior temporal cortex. Details of the density and pattern of terminations from these areas at the light microscopic level were described in a recent study (Barbas *et al.*, 2005). The present analysis is restricted to the ultrastructural level, and focused on layer I, and the middle layers (IV and upper V; Fig. 1*C*), which differ in their corticocortical connections.

BDA labels some neurons retrogradely, raising the possibility that some synapses may be from axons of retrogradely labeled projection neurons. However, retrograde labeling over long distances and long survival times is present mainly in the cell body and dendrites, and there is no evidence that it enters collateral axons (e.g. Wouterlood and Jorritsma-Byham, 1993). Label in the superior temporal cortices was seen mostly in axons and their terminals, consistent with the propensity of the 10 000 mol. wt type BDA for anterograde labeling (Veenman *et al.*, 1992; Reiner *et al.*, 2000). The examined blocks did not contain any retrogradely labeled neurons.

2D Analysis

The first investigation of synapses of axons from areas 32 and 10 focused on superior temporal area Ts1 (at its border with area Ts2; Fig. 1*C*). Axons originating in area 32 and area 10 synapsed with neuronal elements in superior temporal gyrus. Labeled
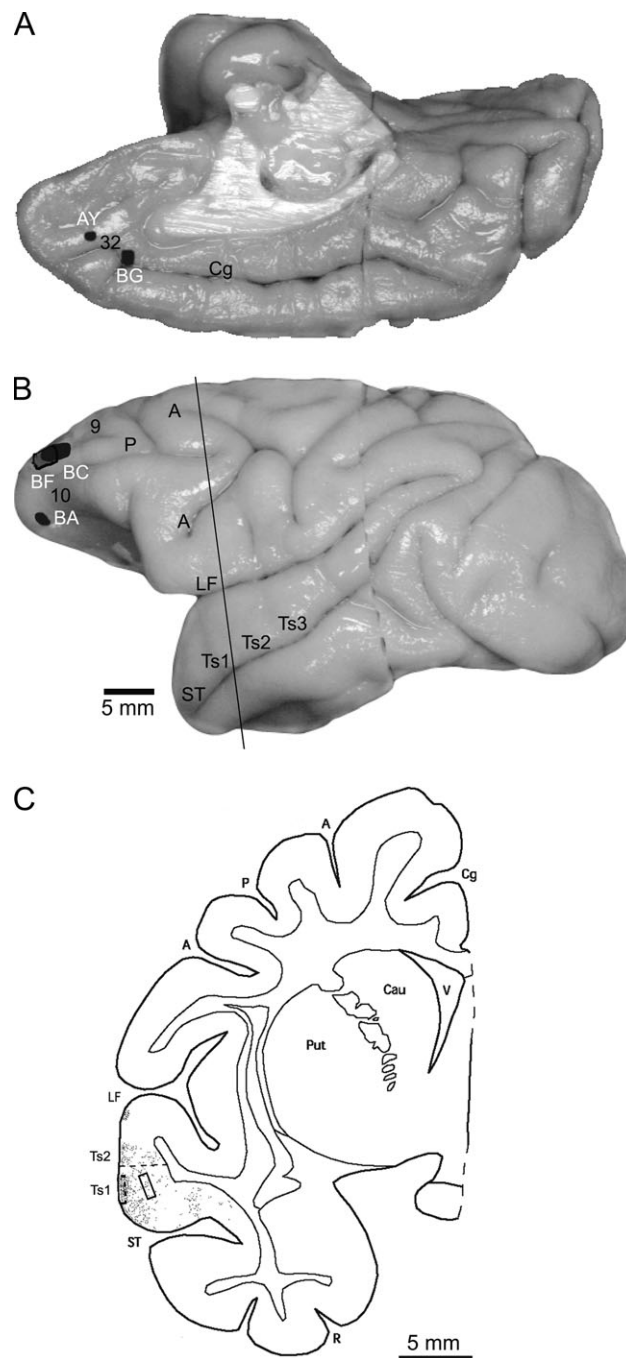
Figure 1. Injection sites and layers used for analysis. (*A*) Injection sites of BDA in medial area 32 in the anterior cingulate shown on the medial surface (cases AY, BG). (*B*) Injection sites in lateral area 10 shown on the lateral surface (cases BA, BC, BF). (*C*) Coronal section taken at the level indicated by vertical line in *B*, showing anterograde labeling in superior temporal areas. The rectangles show the area sampled from layer I (black dotted outline), and the middle layers (IV– upper V, black outline) of area Ts1 for electron microscopic analysis. Abbreviations: A, arcuate sulcus; Cau, caudate; Cg, cingulate sulcus; LF, lateral fissure; P, principal sulcus; Put, putamen; R, rhinal sulcus; ST, superior temporal sulcus; Ts1, Ts2, Ts3, superior temporal areas 1, 2, 3; V, ventricle.

axonal boutons were filled with electron-dense tracer reaction product and formed exclusively asymmetric synapses with distinct postsynaptic densities. Labeled boutons contained small, round synaptic vesicles and mitochondria, neither of which contained label. Labeled boutons synapsed mostly on spines and

to a lesser extent on dendritic shafts. We saw no synapses between labeled boutons and a soma, as seen occasionally in the visual cortical system (e.g. Anderson and Martin, 2002). Examples of synapses involving labeled boutons are shown in Figure 2.

## Synapses of Axons from Area 32 and Area 10 in Superior Temporal Cortex

All synapses between presynaptic boutons from area 32 and postsynaptic elements in superior temporal area Ts1 were asymmetric ($n = 217$). Most synapses involved spines, suggesting that the postsynaptic sites belong to excitatory neurons, consistent with findings in other systems (reviewed in White and Keller, 1989). In layer I labeled terminals formed asymmetric synapses ($n = 113$) mostly with spines (98%) and to a much lesser extent with dendritic shafts (2%). In layers IV–V labeled terminals ($n = 104$) also formed asymmetric synapses with spines (93%) and dendritic shafts (7%), consistent with associational projections in prefrontal cortices in primates (Melchitzky *et al.*, 1998) and rats (Gabbott *et al.*, 2003). The areas of the profiles of labeled boutons synapsing in layer I ($0.32 \pm 0.01~\mu m^2$) were significantly smaller than in layers IV–V ($0.41 \pm 0.01~\mu m^2$) of the superior temporal gyrus ($P = 0.0004$, two tail; Fig. 3A).

We compared data of synapses from axons originating in area 32 with those originating in area 10 (three cases) in superior temporal area Ts1 (cases BA, BC) and in a more caudally situated superior temporal area Ts3 (case BF; Fig. 1). All synapses formed by labeled axonal boutons from area 10 were asymmetric ($n = 336$), and in both layers most were on spines (98%), and only a small number synapsed on dendritic shafts (2%). Again, there were consistent differences in the size of labeled boutons when analyzed by layer, so that profiles of boutons terminating in layers IV–V had significantly larger areas than those terminating in layer I (area for layer I = $0.44 \pm 0.02~\mu m^2$; middle layers = $0.52 \pm 0.02~\mu m^2$; $P = 0.0001$, two tail; Fig. 3A). Consequently, prefrontal boutons synapsing in the middle layers were larger than those synapsing in layer I regardless of prefrontal origin in area 10 or area 32.

We then investigated synaptic features when the origin in prefrontal cortex was in the same area, but the destination differed within the superior temporal gyrus. To address this question we compared synapses made by axons from area 10 in the architectonically distinct superior temporal areas Ts1 and Ts3. As shown in Figure 3B, there were significant differences in the size of boutons between superficial and middle layers for terminations in area Ts1 (cases BA, BC; $n = 244$, $P = 0.035$), as well as in area Ts3 (case BF; $n = 92$, $P = 0.006$).

The differences in bouton size between layer I and the middle layers were noted in female (case BF; $P = 0.006$) as well as in male monkeys (cases BA, BC; $P = 0.035$), for cases with injection in area 10, where both sexes were included. This pattern was also found in the only 3-year-old sexually mature female monkey with tracer injection in area 32 (case AY; $P = 0.0004$), though it is not known whether she was cycling at the time of perfusion,
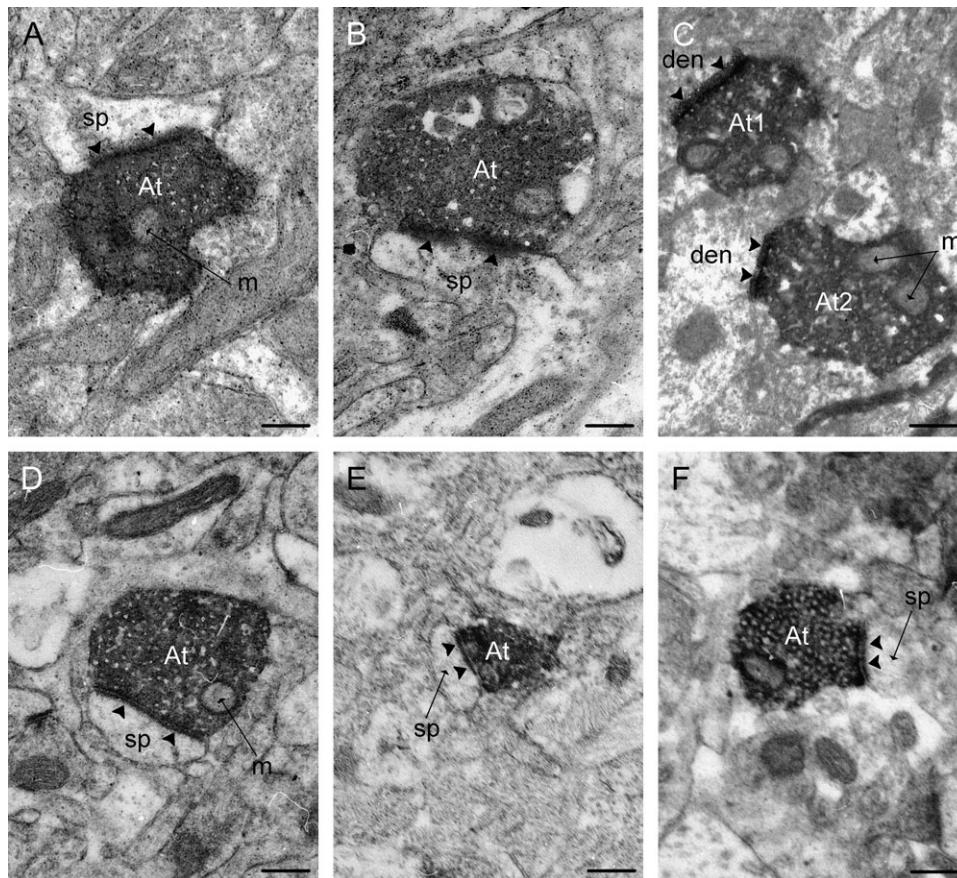
Figure 2. Synapses between prefrontal axons in superior temporal cortex in 2D. (*A–C*) Synapses in the middle layers (layers IV–upper V). (*A, B*) Synapses of labeled boutons (At) on spines (sp). (*C*) Synapses of two distinct boutons (At1, At2) on dendritic shaft (den). (*D, E*) Synapses in layer I were mostly on spines (sp) and boutons were smaller in size overall. Scale bar, 0.25 μm. m, mitochondrion.
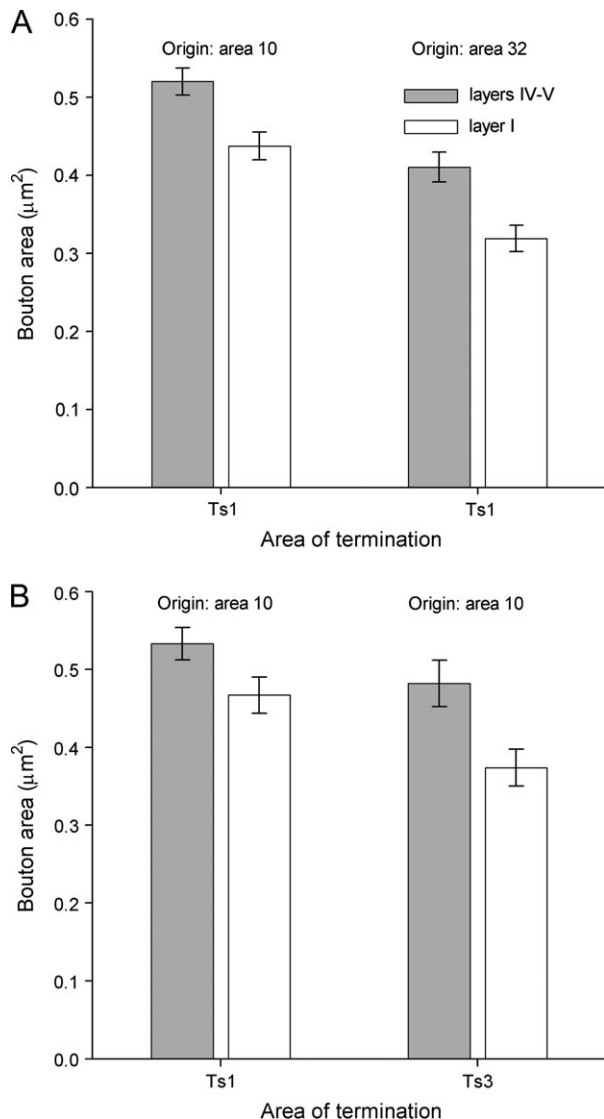
Figure 3. Boutons synapsing in the middle layers (IV–upper V) were larger than those synapsing in layer I of superior temporal cortex. (*A*) Bouton size differences by layer were seen regardless of different origin of axons in lateral prefrontal area 10, or medial (cingulate) area 32. (*B*) Bouton size differences from axons originating in area 10 were noted regardless of their termination in the architectonically distinct superior temporal areas Ts1 and Ts3.

which affects the density of spines in the hippocampus of adult rats (Woolley, 1998). Further study is necessary to determine if presynaptic features of synapses are affected in cycling female rats or monkeys. In addition, the differences in bouton size by layer were found in animals that varied in age, including adolescents (1-2 years of age; cases BA, BF; $P = 0.007$), and young adults (3 years of age; cases BC, AY; $P = 0.0004$). The above evidence suggests that the differences in the size of boutons are not unique to terminations in specific architectonic areas, or to the sex or age of the monkeys within the 1–3 year range examined, but may represent a general pattern in laminar specific corticocortical projections.

We compared the size of labeled versus unlabeled axon terminals at the sites investigated, to determine whether labeled synapses were representative of the surrounding neuropil. In contrast to labeled boutons, there were no differences in the size of unlabeled boutons between layer I ($n = 220$) and the middle layers ($n = 241$), sampled in the vicinity of labeled boutons ($P > 0.05$). Unlabeled boutons represent a heterogeneous group, possibly arising from other cortical or subcortical areas or from local spiny stellate or inhibitory interneurons. The area of profiles of labeled synaptic boutons in the middle layers was larger in the entire group examined (mean = 0.49 μm^2) than in unlabeled synaptic boutons ($n = 220$; mean size = 0.33 μm^2; ANOVA, $P = 0.0003$), a difference seen for each individual case as well. The same trend was seen for the superficial layers for the group (labeled mean size = 0.4 μm^2; unlabeled $n = 241$, mean size = 0.3 μm^2; $P = 0.006$), but only in three of four individual cases tested separately.

3D Reconstruction of Synapses

We conducted a more detailed analysis of labeled and unlabeled synapses using 3D reconstruction in two of the above experiments with labeled pathways from area 10 (cases BC, BF). We aligned 59 series, each consisting of consecutive electron microscope sections in one case (case BC) and 49 series in the second case (case BF) through superior temporal area Ts1 (case BC), and in area Ts3 (case BF; Fig. 1). The tissue was taken from sites close to the sites analyzed in 2D sections (above). From these series we obtained 26 complete reconstructions of labeled boutons from one animal (11 from layer I and 15 from layers IV-V), and 32 reconstructions from another animal (21 in layer I and 11 in layers IV-V). In addition, we reconstructed 31 unlabeled boutons (17 from layer I and 14 from layers IV-V) in the vicinity of labeled boutons, and 58 spines and their postsynaptic densities, which synapsed with both labeled ($n = 34$) and unlabeled boutons ($n = 24$). The internal structure of boutons was visible and we reconstructed mitochondria in 30 boutons (19 labeled and 11 unlabeled).

A vast majority of boutons were ovoid in shape, with their longest axis running parallel to the synaptic cleft (see Fig. 4 for examples). Occasionally, smaller boutons had a spherical shape, but this was rare in the larger boutons. The most common shape was like a kidney bean, although more elaborate shapes were also observed. The structure of the largest boutons often appeared to be shaped by the surrounding neuropil, including dendrites or other postsynaptic elements.

Consistent with the 2D analysis, all synapses formed by labeled boutons (layer I and layers IV-V) were asymmetric and presumably excitatory. In addition, the majority of boutons in the superior temporal cortex formed only single synapses (94% of boutons in layer I; 88% of boutons in layers IV-V). The remaining boutons were generally large and formed two synapses.

Synaptic Targets of Projections

Most reconstructed boutons formed synapses with spines and only a few synapsed with dendritic shafts, but their proportion varied significantly across layers (χ^2, $P = 0.02$). An average of 93% of labeled boutons in layer I formed synapses with spines, and the remainder with dendritic shafts. In contrast, 68% of labeled boutons in layers IV-V formed synapses with spines. The proportion of boutons synapsing on dendritic shafts was somewhat higher than in the 2D analysis (above), perhaps due to the easier distinction between spines and small dendrites in 3D reconstructed synapses.

Reconstruction of post-synaptic elements revealed that when a bouton synapsed with a dendritic shaft, several other boutons
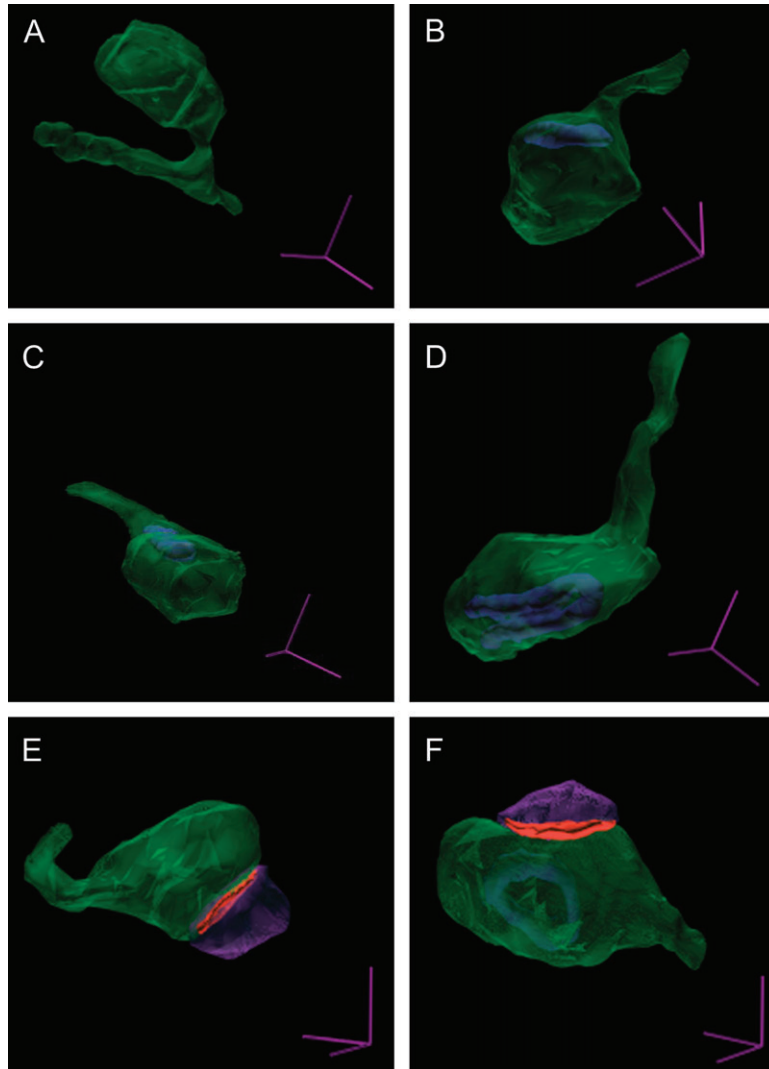
Figure 4. Reconstructed boutons and synapses in 3D. (*A, B*) Reconstructed boutons (green) in layer I without (*A*), and with (*B*) mitochondria (blue). (*C, D*) Reconstructed boutons in layers IV–V. (*E, F*) Reconstructed boutons in layer I (*E*) and IV–V (*F*) synapsing with spines (purple), showing the postsynaptic density (red). Scale bar = 0.5 μm.

synapsed with the same smooth dendritic shaft, suggesting that the postsynaptic target is an inhibitory interneuron. Some labeled boutons formed synapses with shafts of spiny dendrites as well, which had multiple spiny protrusions and few other, if any, synapses on their shafts. Spines and their associated spiny dendrites primarily belong to excitatory neurons (Grey, 1959; Peters *et al.*, 1991). Of the synapses with dendritic shafts that were clearly classifiable, approximately two-thirds were on smooth dendrites, so that 97% of synapses in layer I were made with elements of excitatory neurons, compared with 83% of synapses in layers IV–V. Employing Yates' chi-square correction for low-frequency events, there were no significant differences between the targets in each layer. The same trend was observed in the rat visual cortex (Gonchar and Burkhalter, 2003), and in the middle layers of the cat visual cortical system (Lowenstein and Somogyi, 1991).

Reconstructed spines which formed synapses with labeled boutons had an average volume of 0.0515 μm^3 in layer I, and 0.0540 μm^3 in layers IV–V, and did not differ significantly across layers (*P* = 0.8). Spine volumes were proportional to post-synaptic density (PSD) area (R^2 = 0.82, *P* = 0.0001), as shown in Figure 5, which is consistent with the data reported previously in rat hippocampus (Harris and Stevens, 1989; Schikorski and Stevens, 1999). The relationship of the area of the PSD and spine volume did not differ across layers. The synaptic area was 0.15 ± 0.12 (SD) μm^2 for layer I, and 0.15 ± 0.07 (SD) μm^2 for layers IV–V, comparable to the values obtained in monkey cortical visual pathways (Anderson *et al.*, 1998). In contrast, the postsynaptic density in layers II-III was reported to be smaller than in layer IV in the V2 to MT pathway in macaque monkeys (Anderson and Martin, 2002).

Presynaptic Variability

In contrast to the relative uniformity of dendritic spines across the layers, average labeled bouton volume was heavily dependent on laminar termination, differing significantly between layer I and layers IV–V (*P* = 0.0001; Fig. 6*A*,*B*). Boutons in layers IV-V had a mean volume of 0.339 μm^3, more than twice the volume of boutons in layer I (0.154 μm^3). The probability
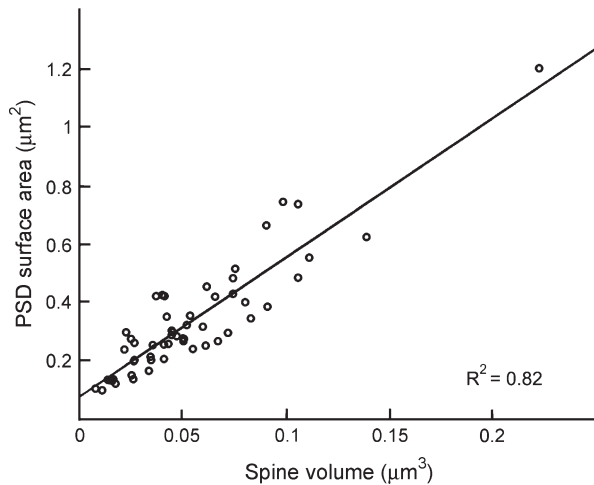
Figure 5. The relationship of spine volume to postsynaptic density (PSD) surface area was linear. The scatter plot includes data from layer I and the middle layers (IV–upper V) which did not differ in this respect.
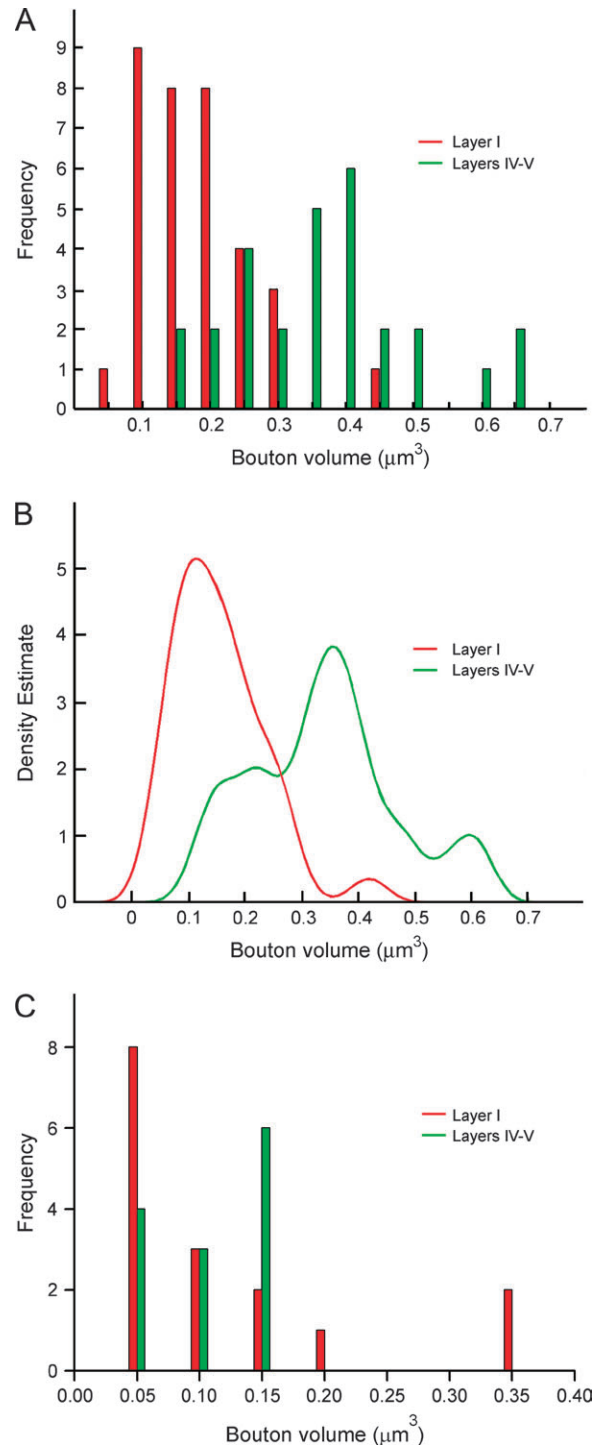
density estimate of bouton volumes suggests that there are three populations of boutons from prefrontal axons terminating in superior temporal cortex (Fig. 6*B*). In contrast, the volumes of unlabeled boutons in layer I (0.116 μm^3) and in layers IV–V (0.101 μm^3) did not differ significantly, showing largely overlapping distributions (Fig. 6*C*).

Bouton Content

To examine the implications of different bouton volumes we investigated whether the principal contents of boutons were related to their volume. The volumes of mitochondria in boutons were linearly related to bouton volumes ($R^2 = 0.70$, $P = 0.0001$), in line with findings in the bullfrog (Lysakowski *et al.*, 1999), rat spinal cord (Vaughn and Grieshaber, 1972) and cat ventral horn (Pierce and Mendell, 1993). Linear regression showed that in the superior temporal cortex, on average, mitochondria constituted 8% of a bouton's volume. Figure 7 shows a scatter plot of this relationship, which is consistent across layers for labeled and unlabeled boutons alike. Labeled reconstructed boutons with mitochondria are shown in Figure 4.

However, not all labeled boutons contained mitochondria. In particular, some of the smallest boutons generally found in layer I, contained no mitochondria, as shown in Figure 4*A,E*. To rule out any influence of BDA staining on these observations, we examined a random sample of unlabeled boutons. Approximately 66% of labeled boutons and 53% of unlabeled boutons in layer I contained no mitochondria. In contrast, only 8% of labeled and 44% of unlabeled boutons in layers IV–V had no mitochondria.

We then examined the relationship between bouton volume and vesicle number. On the basis of vesicle diameters we estimated vesicle numbers using Abercrombie's correction (Abercrombie, 1946). The relationship between bouton volume and vesicle number was linear ($R^2 = 0.79$, $P = 0.0001$; Fig. 8), consistent with previous studies in other species (Yeow and Peterson, 1991; Pierce and Mendell, 1993). We estimated that the average bouton in layer I contains ~180 vesicles, while the average bouton in layers IV–V contains ~350 vesicles. In addition, the diameters of vesicles in layers IV–V (25.8 nm)


Figure 6. Laminar differences in the size of labeled boutons. (*A*) The distribution of labeled boutons in layer I (red) is shifted to the left, and for layers IV–V (green) is shifted to the right. (*B*) Density estimate of labeled boutons volumes in layer I and layers IV–V. The estimate suggests three classes of boutons by size, with the larger classes found predominantly in the middle layers, and the smallest class found mostly in layer I. (*C*) There were no significant differences in the size of unlabeled boutons in layers I and IV–V.

were significantly bigger than in layer I (23.4 nm) ($P = 0.02$). Layer I vesicles occupied an average volume of 6.7×10^{-6} μm^3, compared to an average volume of 9×10^{-6} μm^3 for vesicles in layer IV–V.
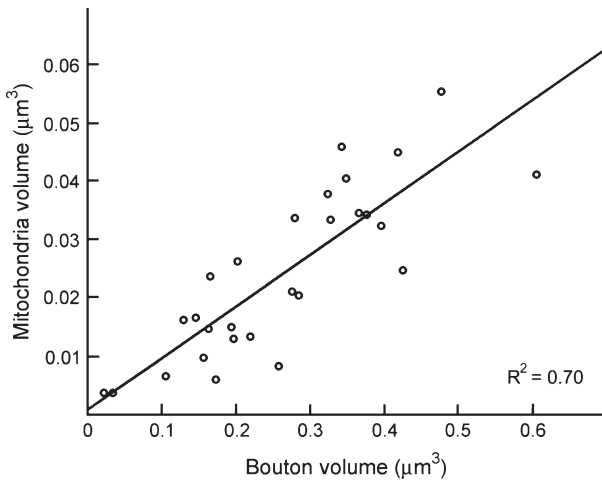
Figure 7. The relationship of bouton volume to mitochondrial volume was linear. The scatter plot includes data from layer I and the middle layers, which did not differ in this respect.
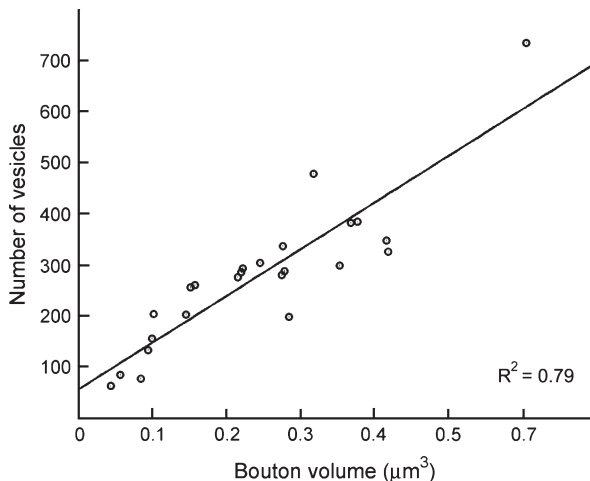
Figure 8. The relationship of bouton volume to vesicular content was linear for boutons in layer I and in the middle layers.

Relationship between Presynaptic and Postsynaptic Elements

In view of the observed dependence of labeled bouton volume on their layer of termination we investigated the relationship between bouton volume and spine volume, a relationship thought to be linear (Harris and Stevens, 1989). However, a linear regression of bouton volume with associated spine volumes showed no significant relationship ($R^2 = 0.046$, $P = 0.277$). We reasoned that the lack of correlation could be explained by large boutons forming more synapses, rather than larger synapses. Including only those boutons that formed a single synapse revealed a significant linear relationship between bouton size and spine volume ($R^2 = 0.18$, $P = 0.02$). However, differences in spine volume accounted for only 18% of the variation in bouton volume. Moreover, the relationship of bouton volume and PSD surface area was not significant ($P = 0.227$). This evidence suggests a degree of independence in the size of presynaptic and postsynaptic elements, so that large boutons are not necessarily associated with large spines.

Discussion

The present data revealed a previously unknown presynaptic specificity in long-distance prefrontal corticocortical pathways. Presynaptic boutons from prefrontal axons synapsing in the middle layers were significantly larger than those in layer I of temporal association cortex, and differed in a number of other ways. The differences in bouton size by layer were evident within one cortical column, and were independent of topographic origin in prefrontal cortex, termination in superior temporal gyrus, or functional attributes of these pathways in behavior.

Postsynaptic Targets of Prefrontal Pathways in Superior Temporal Cortex

Prefrontal pathways terminating in superior temporal areas synapsed mostly with spines, which are found on excitatory neurons, and are particularly enriched on dendrites of neurons in association cortices (e.g. Elston *et al.*, 2001). The considerably less prevalent synapses with dendritic shafts were more common in layers IV–V than in layer I, consistent with previous studies (Jones and Powell, 1970; Johnson and Burkhalter, 1996). Moreover, most synapses involving dendritic shafts were positively identified in serial sections to belong to smooth dendrites, which are characteristic of inhibitory neurons. This finding is consistent with previous anatomic and physiologic findings in the rat visual cortex (Shao and Burkhalter, 1996; Gonchar and Burkhalter, 2003). In contrast, postsynaptic density and shape or volume of spines did not differ significantly between layers I and IV–V. Moreover, we did not see the large variety of spine shapes reported for the monkey cortical visual system (e.g. Anderson *et al.*, 1998; Anderson and Martin, 2002). In the glutamatergic system, synaptic efficacy at the level of the postsynaptic site is dependent on content of AMPA and NMDA receptors and spine shape (Matus, 2000; Matsuzaki *et al.*, 2001). Further study is necessary to determine whether the ratio of AMPA to NMDA receptors differentiates between dendritic spines in layers I and IV–V in the prefrontal-temporal pathway.

Presynaptic Specificity of Prefrontal-temporal Pathways

The most salient discriminant of synapses across layers in the prefrontal-temporal pathway was at the presynaptic level, notably in bouton size. In all cases, labeled boutons from prefrontal axons terminating in the middle layers were significantly larger than boutons in layer I and contained significantly more synaptic vesicles.

The mitochondrial content of labeled boutons was linearly related to bouton volume, in accordance with previous studies (Vaughn and Grieshaber, 1972; Pierce and Mendell, 1993; Pierce and Lewin, 1994; Shepherd and Harris, 1998). In contrast, the average mitochondrial content was less than half of what is reported in the rat and cat spinal cord, in the monkey V1–V5 pathway, or in the cat geniculocortical system (Vaughn and Grieshaber, 1972; Friedlander *et al.*, 1991; Pierce and Mendell, 1993; Anderson *et al.*, 1998). Mitochondrial content is activity dependent (reviewed in Thomson, 2000), suggesting that the prefrontal-temporal pathway is less active than either cortical visual or spinal motor systems. This finding is consistent with the role of the prefrontal cortex in selecting only information that is relevant for the task at hand, suggesting phasic activation of its pathways. Moreover, a significant number of small boutons (<0.4 μm^3) lacked mitochondria. Similar findings have been

reported for boutons in area CA1 of rat hippocampus (Harris and Sultan, 1995; Shepherd and Harris, 1998) which are also small (0.125 ± 0.144 μm³), and in rat visual pathways (Gonchar and Burkhalter, 1999). In contrast, large boutons (>0.45 μm³) in the cat or rat spinal cord (Vaughn and Grieshaber, 1972; Pierce and Mendell, 1993), or in the monkey V1–V5 pathway (Anderson *et al.*, 1998) always contained mitochondria.

Mitochondria have an essential role in energy production by oxidative phosphorylation, raising the question as to how boutons without mitochondria function. Shepherd and Harris (1998) have suggested that ATP may diffuse from the axon, or mitochondria may travel to sites of high metabolic demand along the axon. In our material, some mitochondria extended between the axon and bouton, consistent with the latter view (Fig. 4C). Another possibility is that boutons without mitochondria may be supported by non-oxidative glucose metabolism, as shown in the visual cortex in humans (Fox and Raichle, 1986; Fox *et al.*, 1988). Furthermore, our findings may help explain the difference between the theoretical and measured values for the oxygen-to-glucose index (Shulman *et al.*, 2001).

Theoretical Implications of Laminar-specific Presynaptic Features

Differences in the size of boutons by layer may affect neural dynamics. At the molecular level, it is thought that the size of the releaseable pool of vesicles is directly related to the size of the reserve pool, and the size of the releaseable pool is proportional to release probability (Rosenmund and Stevens, 1996; Ryan *et al.*, 1996; Murthy *et al.*, 1997; see also Walmsley *et al.*, 1998; Stevens, 2003). The greater capacity for synaptic vesicles in labeled boutons in layers IV–V demonstrated here, suggests potentially increased synaptic efficacy in this laminar-specific pathway.

Synaptic efficacy can be inferred, in part, by the quantal excitatory postsynaptic current (EPSC), which is thought to be linearly related to vesicle volume (Karunanithi *et al.*, 2002). In our material, vesicles in layers IV–V were consistently larger than in layer I, and we estimated the possible EPSC for each based on the data of Ventriglia and Di Maio (2003) for AMPA and NMDA receptors in rat hippocampus. In its simplest form (assuming that the released vesicle is in the center of the active zone), Ventriglia and Di Maio's model is strictly linear (R^2 = 0.998). Applying this linear relationship to our data (inner vesicle radius of 11.7 nm in layer I; 12.9 nm in layers IV–V) yielded quantal EPSCs of ~21 pA in layer I, and ~22 pA in layers IV–V, reflecting only a small difference. However, in the visual cortical system, activation of pathways terminating in the middle layers evoke EPSPs of almost twice the amplitude of pathways terminating in layer I (Shao and Burkhalter, 1996), though the number of synapses involved in each pathway is unknown.

Oertner *et al.* (2002) proposed that the amount of neurotransmitter released is proportional to release probability, and multivesicular release from one synapse can release a variable amount of glutamate per action potential (Tong and Jahr, 1994). By that reasoning, the larger boutons from prefrontal axons terminating in layers IV–V are more likely to undergo multivesicular release than boutons in layer I.

What Factors Underlie Differences in Laminar-specific Terminations?

Differences in the size of boutons synapsing in distinct layers may reflect differences in their laminar origin. In this study, the laminar origin of neurons giving rise to the projections is unknown, as the injection site in prefrontal areas encompassed all layers. However, in primates, axons terminating in the middle layers originate mainly from neurons in layer III, whereas axons terminating in layer I originate mostly from neurons in the deep layers (lower part of V and layer VI) (reviewed in Felleman and Van Essen, 1991; Barbas *et al.*, 2002). Boutons from axons originating in area 10 fell into three populations by size, suggesting that several cortical layers may contribute to the projection system according to rules underlying corticocortical connections in a wide variety of systems and species (for review see Felleman and Van Essen, 1991).

In rats, projections originating from primary visual area V1 and terminating in II/III of visual association area LM have larger boutons than projections proceeding in the opposite direction (Gonchar and Burkhalter, 1999). This finding in rats was attributed to differences between feedforward (V1 to LM) and feedback (LM to V1) projections, but is also consistent with differences between distinct pathways. The latter interpretation is consistent with our findings showing overall differences in the size of boutons originating in area 32 compared to area 10, both of which synapsed in anterior superior temporal cortex (see Fig. 3).

A related unanswered question is whether terminations in multiple layers of a given pathway in sensory cortices differ in size by layer within the same cortical column, as our data show for prefrontal-temporal pathways. Addressing this question would directly test the widely held assumption that directionally specific (feedforward and feedback) cortical pathways differ qualitatively (for review see Felleman and Van Essen, 1991). An alternative explanation is that connections differ quantitatively, and this is supported by evidence in several cortical systems (e.g. Schwartz and Goldman-Rakic, 1984; Barbas, 1986; De Lima *et al.*, 1990; Einstein, 1996). Further, the relative laminar distribution of connections varies consistently in a graded pattern that can be predicted by the gross laminar features of the linked areas, according to the rules of the structural model for connections (Barbas and Rempel-Clower, 1997). This model is independent of direction, it can be applied to sensory as well as other cortical systems, and accurately describes the laminar pattern of diverse cortical connections (e.g. Barbas *et al.*, 1999; Rempel-Clower and Barbas, 2000), including prefrontal-superior temporal pathways (Barbas *et al.*, 2005). In principle, the density and pattern of terminations of pathways in distinct layers may be used to model the strength of pathways and their interaction with laminar-specific excitatory and inhibitory systems (Barbas *et al.*, 2005). The present findings demonstrate a novel feature in these pathways by distinguishing at the synaptic level terminations in the middle layers from those terminating in layer I. These findings may help characterize 'driver' from 'modulatory' pathways in corticocortical pathways, as suggested for thalamocortical pathways (Ahmed *et al.*, 1997; Crick and Koch, 1998; Sherman and Guillery, 1998).

Presynaptic features undergo structural changes in development, or in response to a variety of physiological triggers (e.g. Friedlander and Martin, 1989; Ma *et al.*, 1999; Hatada *et al.*, 2000; Nikonenko *et al.*, 2003; reviewed in Fitzsimonds and Poo, 1998; White, 2002; Chklovskii *et al.*, 2004). Our findings indicate robust presynaptic differences at the laminar level in adult primates, which are likely sculpted through experience. The absence of mitochondria in small boutons which are most prevalent in layer I suggests the intriguing possibility of differences in metabolic regulation in laminar specific pathways.

The potential generality of these novel findings remains to be tested in other cortical systems. Nevertheless, the laminar-specific presynaptic differences in prefrontal-temporal pathways were independent of specific origin in prefrontal cortex, destination in superior temporal cortex, or functional attributes in behavior.

Notes

Address correspondence to Helen Barbas, Boston University, 635 Commonwealth Avenue, Room 431, Boston, MA 02215, USA. Email: barbas@bu.edu.

References

Abercrombie M (1946) Estimation of nuclear population from microtome sections. Anat Rec 94:239-247.

Ahmed B, Anderson JC, Martin KA, Nelson JC (1997) Map of the synapses onto layer 4 basket cells of the primary visual cortex of the cat. J Comp Neurol 380:230-242.

Anderson JC, Martin KA (2002) Connection from cortical area V2 to MT in macaque monkey. J Comp Neurol 443:56-70.

Anderson JC, Binzegger T, Martin KAC, Rockland KS (1998) The connection from cortical area V1 to V5: a light and electron microscopic study. J Neurosci 18:10525-10540.

Archambeaum C, Verleysen M (2003) Fully nonparametric probability density function estimation with finite Gaussian mixture models. ICAPR Proc 5:81-84.

Barbas H (1986) Pattern in the laminar origin of corticocortical connections. J Comp Neurol 252:415-422.

Barbas H, Rempel-Clower N (1997) Cortical structure predicts the pattern of corticocortical connections. Cereb Cortex 7:635-646.

Barbas H, Ghashghaei H, Dombrowski SM, Rempel-Clower NL (1999) Medial prefrontal cortices are unified by common connections with superior temporal cortices and distinguished by input from memory-related areas in the rhesus monkey. J Comp Neurol 410:343-367.

Barbas H, Ghashghaei H, Rempel-Clower N, Xiao D (2002) Anatomic basis of functional specialization in prefrontal cortices in primates. In: Handbook of Neuropsychology (Grafman, J, ed), pp. 1-27. Amsterdam: Elsevier Science B. V.

Barbas H, Medalla M, Alade O, Suski J, Zikopoulos B, Lera P. (2005) Relationship of prefrontal connections to inhibitory systems in superior temporal areas in the rhesus monkey. Cereb Cortex 15:1356-1370.

Chao LL, Knight RT (1997) Prefrontal deficits in attention and inhibitory control with aging. Cereb Cortex 7:63-69.

Chao LL, Knight RT (1998) Contribution of human prefrontal cortex to delay performance. J Cogn Neurosci 10:167-177.

Chklovskii DB, Mel BW, Svoboda K (2004) Cortical rewiring and information storage. Nature 431:782-788.

Crick F, Koch C (1998) Constraints on cortical and thalamic projections: the no-strong-loops hypothesis. Nature 391:245-250.

De Lima AD, Voigt T, Morrison JH (1990) Morphology of the cells within the inferior temporal gyrus that project to the prefrontal cortex in the macaque monkey. J Comp Neurol 296:159-172.

Einstein G (1996) Reciprocal projections of cat extrastriate cortex: I. Distribution and morphology of neurons projecting from posterior medial lateral suprasylvian sulcus to area 17. J Comp Neurol 376:518-529.

Elston GN, Benavides-Piccione R, DeFelipe J (2001) The pyramidal cell in cognition: a comparative study in human and monkey. J Neurosci 21:RC163.

Felleman DJ, Van Essen DC (1991) Distributed hierarchical processing in the primate cerebral cortex. Cereb Cortex 1:1-47.

Fiala JC, Harris KM (1999) Dendrite Structure. In: Dendrites (Stuart G, Spruston N, Häusser M, eds), pp. 1-34. Oxford: Oxford University Press.

Fiala JC, Harris KM (2001) Cylindrical diameters method for calibrating section thickness in serial electron microscopy. J Microsc 202: 468-472.

Fiala JC, Harris KM (2002) PC-based alignment and reconstruction of serial sections. Microsc Anal 52:5-7.

Fitzsimonds RM, Poo MM (1998) Retrograde signaling in the development and modification of synapses. Physiol Rev 78:143-170.

Fox GQ (1988) A morphometric analysis of synaptic vesicle distributions. Brain Res 475:103-117.

Fox PT, Raichle ME (1986) Focal physiological uncoupling of cerebral blood flow and oxidative metabolism during somatosensory stimulation in human subjects. Proc Natl Acad Sci USA 83:1140-1144.

Fox PT, Raichle ME, Mintun MA, Dence C (1988) Nonoxidative glucose consumption during focal physiologic neural activity. Science 241:462-464.

Friedlander MJ, Martin KAC (1989) Development of γ-axon innervation of cortical area 18 in the cat. J Physiol 416:182-213.

Friedlander MJ, Martin KA, Wassenhove-McCarthy D (1991) Effects of monocular visual deprivation on geniculocortical innervation of area 18 in cat. J Neurosci 11:3268-3288.

Froesch D (1973) A simple method to estimate the true diameter of synaptic vesicles. J Microsc 98:85-89.

Gabbott PL, Warner TA, Jays PR, Bacon SJ (2003) Areal and synaptic interconnectivity of prelimbic (area 32), infralimbic (area 25) and insular cortices in the rat. Brain Res 993:59-71.

Gonchar Y, Burkhalter A (1999) Differential subcellular localization of forward and feedback interareal inputs to parvalbumin expressing GABAergic neurons in rat visual cortex. J Comp Neurol 406:346-360.

Gonchar Y, Burkhalter A (2003) Distinct GABAergic targets of feedforward and feedback connections between lower and higher areas of rat visual cortex. J Neurosci 23:10904-10912.

Grey EG (1959) Electron microscopy of synaptic contacts on dendrite spines of the cerebral cortex. Nature 183:1592-1593.

Guillery RW, Herrup K (1997) Quantification without pontification: choosing a method for counting objects in sectioned tissues. J Comp Neurol 386:2-7.

Harris KM, Stevens JK (1989) Dendritic spines of CA 1 pyramidal cells in the rat hippocampus: serial electron microscopy with reference to their biophysical characteristics. J Neurosci 9:2982-2997.

Harris KM, Sultan P (1995) Variation in the number, location and size of synaptic vesicles provides an anatomical basis for the nonuniform probability of release at hippocampal CA1 synapses. Neuropharmacology 34:1387-1395.

Hatada Y, Wu F, Sun ZY, Schacher S, Goldberg DJ (2000) Presynaptic morphological changes associated with long-term synaptic facilitation are triggered by actin polymerization at preexisting varicosities. J Neurosci 20:RC82.

Hof PR, Glezer II, Conde F, Flagg RA, Rubin MB, Nimchinsky EA, Vogt Weisenhorn DM (1999) Cellular distribution of the calcium-binding proteins parvalbumin, calbindin, and calretinin in the neocortex of mammals: phylogenetic and developmental patterns. J Chem Neur 16:77-116.

Johnson RR, Burkhalter A (1996) Microcircuitry of forward and feedback connections within rat visual cortex. J Comp Neurol 368:383-398.

Jones EG, Powell TP (1970) An electron microscopic study of the laminar pattern and mode of termination of afferent fibre pathways in the somatic sensory cortex of the cat. Philos Trans R Soc Lond B Biol Sci 257:45-62.

Karunanithi S, Marin L, Wong K, Atwood HL (2002) Quantal size and variation determined by vesicle size in normal and mutant Drosophila glutamatergic synapses. J Neurosci 22:10267-10276.

Koechlin E, Basso G, Pietrini P, Panzer S, Grafman J (1999) The role of the anterior prefrontal cortex in human cognition. Nature 399:148-151.

Lowenstein PR, Somogyi P (1991) Synaptic organization of corticocortical connections from the primary visual cortex to the posteromedial lateral suprasylvian visual area in the cat. J Comp Neurol 310:253-266.

Lund JS (1988) Anatomical organization of macaque monkey striate visual cortex. Annu Rev Neurosci 11:253-288.

Lysakowski A, Figueras H, Price SD, Peng YY (1999) Dense-cored vesicles, smooth endoplasmic reticulum, and mitochondria are closely associated with non-specialized parts of plasma membrane of nerve terminals: implications for exocytosis and calcium buffering by intraterminal organelles. J Comp Neurol 403:378–390.

Ma L, Zablow L, Kandel ER, Siegelbaum SA (1999) Cyclic AMP induces functional presynaptic boutons in hippocampal CA3-CA1 neuronal cultures. Nat Neurosci 2:24–30.

Matsuzaki M, Ellis-Davies GC, Nemoto T, Miyashita Y, Iino M, Kasai H (2001) Dendritic spine geometry is critical for AMPA receptor expression in hippocampal CA1 pyramidal neurons. Nat Neurosci 4:1086–1092.

Matus A (2000) Actin-based plasticity in dendritic spines. Science 290:754–758.

Melchitzky DS, Sesack SR, Pucak ML, Lewis DA (1998) Synaptic targets of pyramidal neurons providing intrinsic horizontal connections in monkey prefrontal cortex. J Comp Neurol 390:211–224.

Murthy VN, Sejnowski TJ, Stevens CF (1997) Heterogeneous release properties of visualized individual hippocampal synapses. Neuron 18:599–612.

Nikonenko I, Jourdain P, Muller D (2003) Presynaptic remodeling contributes to activity-dependent synaptogenesis. J Neurosci 23: 8498–8505.

Oertner TG, Sabatini BL, Nimchinsky EA, Svoboda K (2002) Facilitation at single synapses probed with optical quantal analysis. Nat Neurosci 5:657–664.

Peters A, Palay SL, Webster HD (1991) The fine structure of the nervous system. Neurons and their supporting cells. New York: Oxford University Press.

Pierce JP, Mendell LM (1993) Quantitative ultrastructure of Ia boutons in the ventral horn: scaling and positional relationships. J Neurosci 13:4748–4763.

Pierce JP, Lewin GR (1994) An ultrastructural size principle. Neuroscience 58:441–446.

Reiner A, Veenman CL, Medina L, Jiao Y, Del Mar N, Honig MG (2000) Pathway tracing using biotinylated dextran amines. J Neurosci Methods 103:23–37.

Rempel-Clower NL, Barbas H (2000) The laminar pattern of connections between prefrontal and anterior temporal cortices in the rhesus monkey is related to cortical structure and function. Cereb Cortex 10:851–865.

Rosene DL, Roy NJ, Davis BJ (1986) A cryoprotection method that facilitates cutting frozen sections of whole monkey brains from histological and histochemical processing without freezing artifact. J Histochem Cytochem 34:1301–1315.

Rosenmund C, Stevens CF (1996) Definition of the readily releasable pool of vesicles at hippocampal synapses. Neuron 16:1197–1207.

Ryan TA, Li L, Chin LS, Greengard P, Smith SJ (1996) Synaptic vesicle recycling in synapsin I knock-out mice. J Cell Biol 134:1219–1227.

Schikorski T, Stevens CF (1999) Quantitative fine-structural analysis of olfactory cortical synapses. Proc Natl Acad Sci USA 96:4107–4112.

Schmitz C, Hof PR (2005) Design-based stereology in neuroscience. Neuroscience 130:813–831.

Schwartz ML, Goldman-Rakic PS (1984) Callosal and intrahemispheric connectivity of the prefrontal association cortex in rhesus monkey: Relation between intraparietal and principal sulcal cortex. J Comp Neurol 226:403–420.

Shao Z, Burkhalter A (1996) Different balance of excitation and inhibition in forward and feedback circuits of rat visual cortex. J Neurosci 16:7353–7365.

Shepherd GM, Harris KM (1998) Three-dimensional structure and composition of CA3→CA1 axons in rat hippocampal slices: implications for presynaptic connectivity and compartmentalization. J Neurosci 18:8300–8310.

Sherman SM, Guillery RW (1998) On the actions that one nerve cell can have on another: distinguishing 'drivers' from 'modulators'. Proc Natl Acad Sci USA 95:7121–7126.

Shulman RG, Hyder F, Rothman DL (2001) Cerebral energetics and the glycogen shunt: neurochemical basis of functional imaging. Proc Natl Acad Sci USA 98:6417–6422.

Stevens CF (2003) Neurotransmitter release at central synapses. Neuron 40:381–388.

Thomson AM (2000) Molecular frequency filters at central synapses. Prog Neurobiol 62:159–196.

Tong G, Jahr CE (1994) Multivesicular release from excitatory synapses of cultured hippocampal neurons. Neuron 12:51-59.

Vaughn JE, Grieshaber JA (1972) An electron microscopic investigation of glycogen and mitochondria in developing and adult rat spinal motor neuropil. J Neurocytol 1:397–412.

Veenman CL, Reiner A, Honig MG (1992) Biotinylated dextran amine as an anterograde tracer for single- and double-labeling studies. J Neurosci Meth 41:239–254.

Ventriglia F, Di Maio V (2003) Stochastic fluctuations of the quantal EPSC amplitude in computer simulated excitatory synapses of hippocampus. Biosystems 71:195–204.

Vogt BA, Barbas H (1988) Structure and connections of the cingulate vocalization region in the rhesus monkey. In: The physiological control of mammalian vocalization (Newman JD, ed.), pp. 203–225. New York: Plenum.

Walmsley B, Alvarez FJ, Fyffe RE (1998) Diversity of structure and function at mammalian central synapses. Trends Neurosci 21:81–88.

White EL (2002) Specificity of cortical synaptic connectivity: emphasis on perspectives gained from quantitative electron microscopy. J Neurocytol 31:195–202.

White EL, Keller A (1989) Cortical circuits. Synaptic organization of the cerebral cortex. Structure, function and theory. Boston, MA: Birkhäuser.

Woolley CS (1998) Estrogen-mediated structural and functional synaptic plasticity in the female rat hippocampus. Horm Behav 34:140–148.

Wouterlood FG, Jorritsma-Byham B (1993) The anterograde neuroanatomical tracer biotinylated dextran-amine: comparison with the tracer *Phaseolus vulgaris*-leucoagglutinin in preparations for electron microscopy. J Neurosci Meth 48:75–87.

Yeow MB, Peterson EH (1991) Active zone organization and vesicle content scale with bouton size at a vertebrate central synapse. J Comp Neurol 307:475–486.